Bio- and Mineral-Fuel Spray Evolution in Non-Evaporating and Evaporating Conditions by Image Processing Techniques

L. Allocca*, E. Mancaruso, A. Montanaro, L. Sequino, B. M. Vaglieco
Istituto Motori CNR
Via G. Marconi 8 – 80125 Napoli - Italy

Abstract

Fuels from renewable resources have obtained an increasing interest for transport application in the last decade because of their biodegradability, potential improvements on exhaust emission and benefits on virtuous CO_2 cycle of the earth. Within this framework, the paper presents the influence of biodiesel fuels on the injection process and their impact on the air-fuel mixture preparation. The results of an experimental investigation on the fuel spray from a multi-jet common rail injection system both under non evaporative and evaporative conditions are illustrated. The characteristics of the investigated spray include the fuel delivery and instantaneous flow rate and the jet visualization, both within a high pressure vessel at ambient temperature and in an optically accessible single cylinder diesel engine for the evaporative conditions.

Images of the spray evolution, under non evaporative conditions, have been captured, in single-shot mode, by a high spatial resolution CCD camera. They have been processed off-line to estimate the spray tip penetration, cone angle and density distribution. Analogous characterization of the injection images have been performed on the data acquired in the combustion chamber of the optical diesel. The spray tip penetration and liquid fuel distribution have been measured for several engine operating conditions and different biodiesels.

The injection profiles appear similar for all the used fuels in terms of pulse slopes and timing distributions. Images recorded in the evaporating system show a negligible variation of the tip penetration for the different fuels dependent on engine condition rather than on fuels properties. Nevertheless a comparison of the tip penetration in evaporative and non evaporative systems has been made. Finally a different spatial distribution of the liquid fuel has been noted analysing the luminous intensity spatial distribution along the jet direction.

Introduction

Alternative fuels for diesel engines are becoming important due to the decrease of petroleum reservoirs and the increase of environment pollution problems [1]. The biodiesel is technically competitive with conventional petroleum-derived diesel fuel and requires virtually no changes in the fuel distribution infrastructure. For this reason and its biodegradability, the use of biodiesel is considered a good alternative to fossil fuels [2]. Moreover, there is evidence that biodiesel, fuelling the engine, can have a strong impact on performances and pollutant emissions. In particular, the last generation electronically controlled diesel engines using biodiesel have shown a decrease in the emission of particulate matter and unburned hydrocarbons. Vice versa, although many researches show a slight increase in NOx emissions when using biodiesel fuel, some others have been found different effects [3]. The feedstock used for the biodiesels production interferes with the human food chain, and the production costs are very high. These are the two main problems of the first generation biodiesel. For this reason, researchers are making considerable efforts in the development of an alternative production path, leading to the so-called second generation of biodiesel. The 1st generation is essentially a blend of methyl-esters while the 2nd are paraffin hydrocarbons [4]. It seems that there is a potential to reduce gaseous and smoke emissions using biodiesel blends, when an engine and its auxiliary systems (fuel injection, EGR) have been optimized for the specific blend.

Injection process of biodiesels influences the atomization and dispersion of the fuel in the combustion chamber. Consequently, the combustion process and the exhaust emissions depend on the mixture preparation during the ignition delay. Researchers worldwide reported the relationship between these processes and chemical characteristics of the fuel/biofuels or their blends studied in quiescent vessel optically accessible [5, 6].

The research activity described in this paper is part of a wider study that involves fuel injection both in cold spray bomb investigations and in single-cylinder engine in order to assess the various biodiesel types on combustion behaviour (including performance, specific fuel consumption, GHG and pollutant emissions). Optical diagnostics based on imaging have been applied both in high-pressure optically accessible quiescent vessel for non-evaporating investigation and in the combustion chamber of a DI diesel engine for evaporating/combustion conditions using two pure biofuels, Soybean Methyl Ester (SME) and Gas To Liquid (GTL). Injection rates have been measured for all the used fuel and the defined injection strategies. The diesel engine has been optically ac-

* Corresponding author: l.allocca@im.cnr.it

cessible through quartz windows and equipped with multivalve head of real engine. The fuel penetration, spray atomization, air/fuel mixing and cone angle have been analyzed in non evaporating and evaporating conditions for multi injection strategies performed with last generation Common Rail (CR) high pressure injection system. It is typical of new generation Euro 5 diesel engines.

Experimental Apparatuses and Procedures

The effects on the injection process of the physical and chemical properties of a commercial diesel and two alternative diesel fuels are the main objective of the present study. The injection process characterization has been carried out under non evaporative conditions injecting the fuel within stagnant inert gas in a high-pressure optically-accessible cylindrical vessel in order to measure the spatial and temporal distribution of the fuel. Moreover, the injection process has been studied in an optically accessible single cylinder Common Rail diesel engine representing evaporative conditions similar to the real engine. The selected engine working condition has been extracted from the ECU map of a commercial EURO 5 engine. They are 1500 rpm at 2 bar of break mean effective pressure (BMEP) and 2000 rpm at 5 bar of BMEP, respectively. The corresponding injection pressures are 50 and 73 MPa. The implemented injection strategy consists of pilot + main pulses and has been fixed for all fuels. A Bosch second-generation common rail system has been used to inject the fuel through a CRI2.2 injector with 7-hole nozzle, 440 cc/30s @100bar flow number, 148 deg cone opening angle (minisac type). First generation of biodiesel, Soybean Methyl Ether (SME), and second one, Gas To Liquid (GTL), have been used and their behaviours have been compared to the reference diesel fuel. A comparison of physical properties of mineral diesel fuel, first and second generation of biodiesels is reported in Table 1.

Table 1. Physical properties of mineral fuel and first and second generation biofuels

Feature	Method	Diesel	GTL	SME
Density @ 15 °C [kg/m3]	EN ISO 12185	840.1	777.5	884.4
Viscosity a 40 °C [mm2/s]	EN ISO 3104	3.141	2.547	3.958
Oxydation Thermal Stability a 110°C h	EN 14112	-	-	7.9
Oxydation stability [g/m3]	EN ISO 12205	0.1	0.8	1.2
Lubricity a 60 °C [micron]	EN ISO 12156-1	-	235	174
Cetane Number	EN ISO 5165	51.8	73.9	48
Net Heat Value [MJ/kg]	ASTM D3338	43.1	43.53	37.25

Non-evaporative experimental setup

The experimental activity has implied the measurement of instantaneous fuel injection rates on suitable test rig and the spatial-temporal evolution of the jets sprayed from the nozzle in a spray bomb.

A Programmable Electronic Control Unit (PECU) controlled the injection apparatus, thus enabling to set the strategies in terms of pulse number and timing. Fast electronic drivers in the PECU has allowed setting precise and stable injections like the one involving small fuel quantities in multiple injections. The high pressure pump supplying the fuel to the CR has been driven by a variable speed electric motor while a heat exchange system on the hydraulic circuit has been adopted to keep a constant fuel temperature in the tank, (21±1 °C).

The fuel injection rate has been measured by an AVL Fuel Injection Gauge Rate System fitted on the Bosch tube inlet. The whole injected fuel per stroke is the integral of the instantaneous fuel rate over the total injection time [7]. The amount of injected fuel obtained has been successfully compared with the one pounded at the Bosch tube discharge by a precision balance.

The spatial and temporal evolution of the injected fuel have been measured by digital processing of spray images captured at different time from the start of injection in an optically-accessible quiescent vessel filled at engine-like gas densities. SF_6 gas (density 6.2 kg/m^3) has been used in the vessel at room temperature reaching the desired gas densities at lower pressures than air. Pressures of 0.28 and 0.36 MPa have been set in order to achieve gas density of 17.5 and 22.6 kg/m^3, respectively. The images of evolving jets have been captured by a VCO - CCD camera (1376x1040 pixels, 12 bit, 0.5 μs shutter time) synchronized both with the injection system and a set of high intensity flashes. The camera has used a 95 mm macro lens for the pilot injection, while a 50 mm lens for the main pulse has allowed the acquisition of images with a field of view capable to cover the complete penetration of the sprays. Several images of consecutive injections have been acquired at each time-step.

The stability and uniformity of the evolving sprays has made these conditions confident with a statistical evaluation on the spread of the parameters under study.

Analysis of the liquid fuel spray images has been carried out by image processing software: image acquisition, background subtraction and filtering, edges determination, tip penetration and cone angle measures. A sketch of experimental apparatus for tests under non evaporative conditions and further details on the analysis procedure has been reported in [8].

Optical Engine

In order to study the spatial and temporal evolution of the fuel jets under the real pressure and temperature conditions a transparent diesel engine has been used. The transparent single-cylinder engine used for optical diagnostics has been equipped with the head and injection system of the four-cylinder, 16 valves, 1.9l, standard production engine.

The optical engine has used a conventionally extended piston with a 46 mm diameter piston crown window. It has provided full view of the combustion bowl by locating an appropriate 45° UV-visible fixed mirror inside the extended piston. The window has been realized with UV-grade fused silica. To compensate for the slightly lower compression ratio typical of the optical engines and to match the in-cylinder conditions of the real multi-cylinder engine, an external air compressor has been used to supply pressurized intake air. The air has been well filtered, dehumidified, and preheated. Moreover, a cooled EGR system has been used, and a pressure valve has been set in the exhaust pipe in order to ensure the correct operation of the burned gas recirculation system. The engine has been equipped with the same common rail (CR) injection system used in non evaporative conditions. More details about the specifications of the engine are reported in [9].

The injector has been controlled by a fully flexible Electronic Control Unit (ECU) for combustion optimization. The intake air pressure has been set to 0.11 MPa @ 1500 rpm and 0.13 MPa @ 2000 rpm. The intake temperature was 323 K. At 1500 rpm, with an injection pressure of 50 MPa, the energizing time (ET) for the pilot has been set to 350 μs for all the fuels. For the main injection the ET has been set to 600 μs for Diesel and GTL and to 640 μs for SME. At 2000 rpm, with an injection pressure of 73 MPa, it has been set, respectively, 260 μs for the pilot, 560 μs for the main injection of Diesel and GTL and 590 μs for SME.

Digital imaging analysis has been performed by a CCD camera through the 45° mirror. The CCD camera with 640 x 480 pixels and a high sensitivity over a wide visible range has been. Two external highly luminous CW halogen lamps have been used to light the spray. All the images have been acquired with an exposure time corresponding to 0.5° crank angle (ca). Images at 1500 rpm have been acquired with an exposure time of 55 μs, while images at 2000 rpm have been acquired with an exposure time of 41 μs. More details and specifications about the optical set-up are reported in ref. [10].

Results

In Table 2 the amount of injected fuel in the pilot pulse and the complete injection are reported for all the tested fuels operating. Due to SME lower energy content with respect to the mineral fuel, the main pulse duration has been increased for achieving equivalent power output. The instantaneous amount of discharged fuel has been derived from the injection pressure peak in the injector adapter on the AVL meter. The total quantity has been obtained by integrating the pressure signal over the injection duration.

Table 2. Pilot pulse and total injected fuel for the different fuels and engine conditions

		DIESEL		GTL		SME	
P_{inj} [MPa]	Inj. time [μs]	pilot [mg/str]	Q_{tot} [mg/str]	pilot [mg/str]	Q_{tot} [mg/str]	pilot [mg/str]	Q_{tot} [mg/str]
50	350_820_600	1.41	7.61	1.52	7.41	-	-
50	350_820_640	-	-	-	-	1.54	8.69
73	260_1120_560	1.05	11.99	0.98	11.55	-	-
73	260_1120_590	-	-	-	-	0.79	13.74

Figure 1 reports the injection rate profiles for the three fuels and for both engine conditions. The profiles have a quite similar behaviour in terms of rise time and slope and no differences appear against the different densities/viscosities of the fuels. The time scale has been chosen setting the initial point at the first fuel exit from the nozzle for the pilot pulse. Consequently, the main injection appears around 1200 μs and 1400 μs after the start of the pilot for the low and high load condition respectively. Each profile is averaged on one hundred shots.

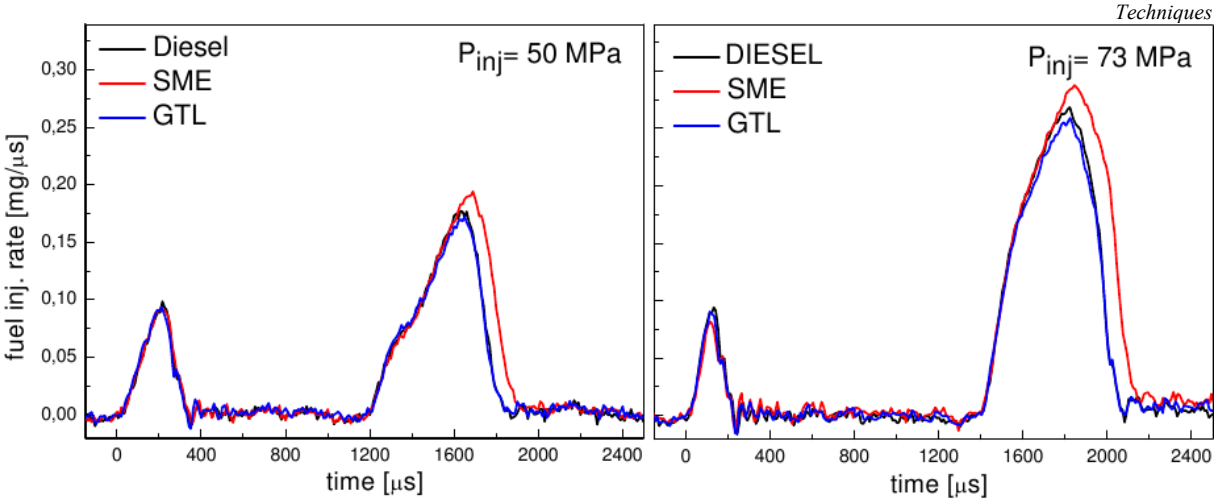

Figure 1. Fuel injection rate profiles for the different investigated fuels and both engine conditions

The spray penetration of the liquid tip has been measured from the edges of the spray as described in the experimental apparatus paragraph. The spray penetration has been considered as the biggest distance of fuel droplet from the nozzle. In this paper the spray penetration is presented as the average of the 7 jets, of which the spray is formed, and 5 images repetitions at the same conditions in order to reduce the intrinsic irregularity of the spray evolution due to the non-uniform flow field within the chamber.

The single and averaged tip penetrations profiles, against time from the injection start, have been analyzed for all fuels. They have initial linear trends with slight differences between sprays, indicating a good stability of the injection process. Figure 2 reports the jets penetration profiles, labelled 'jet1'-'jet7'. The low load condition (P_{inj} 50 MPa) is reported at the left while the high load one (P_{inj} 73 MPa) is at the right. It is worthwhile to note the anisotropy between the jets is negligible in both the working conditions and for the different fuels . Some differences in the jets penetration appear only at the lowest injection pressure and vessel gas density for Diesel and GTL main pulse. It is due to their lowest density and viscosity. At the highest load the fuel penetration process is more stable and less dependent on chemical-physical properties of the fuels. In Figure 3 has been reported the tip penetration for each jet in non evaporative system, at P_{inj} of 50 MPa using GTL fuel for different time. At each injection times are evident the different penetration values of the seven jets.

The trends of the averaged penetrations are quite linear and similar both for the pilot and the main injection. The jets averaged penetration profiles almost overlap for all tested conditions. Some differences appear at the end of the curves when the effect of the fuel momentum decreases. This behaviour has been confirmed for all fuel types. This phenomenon is independent on their density/viscosity.

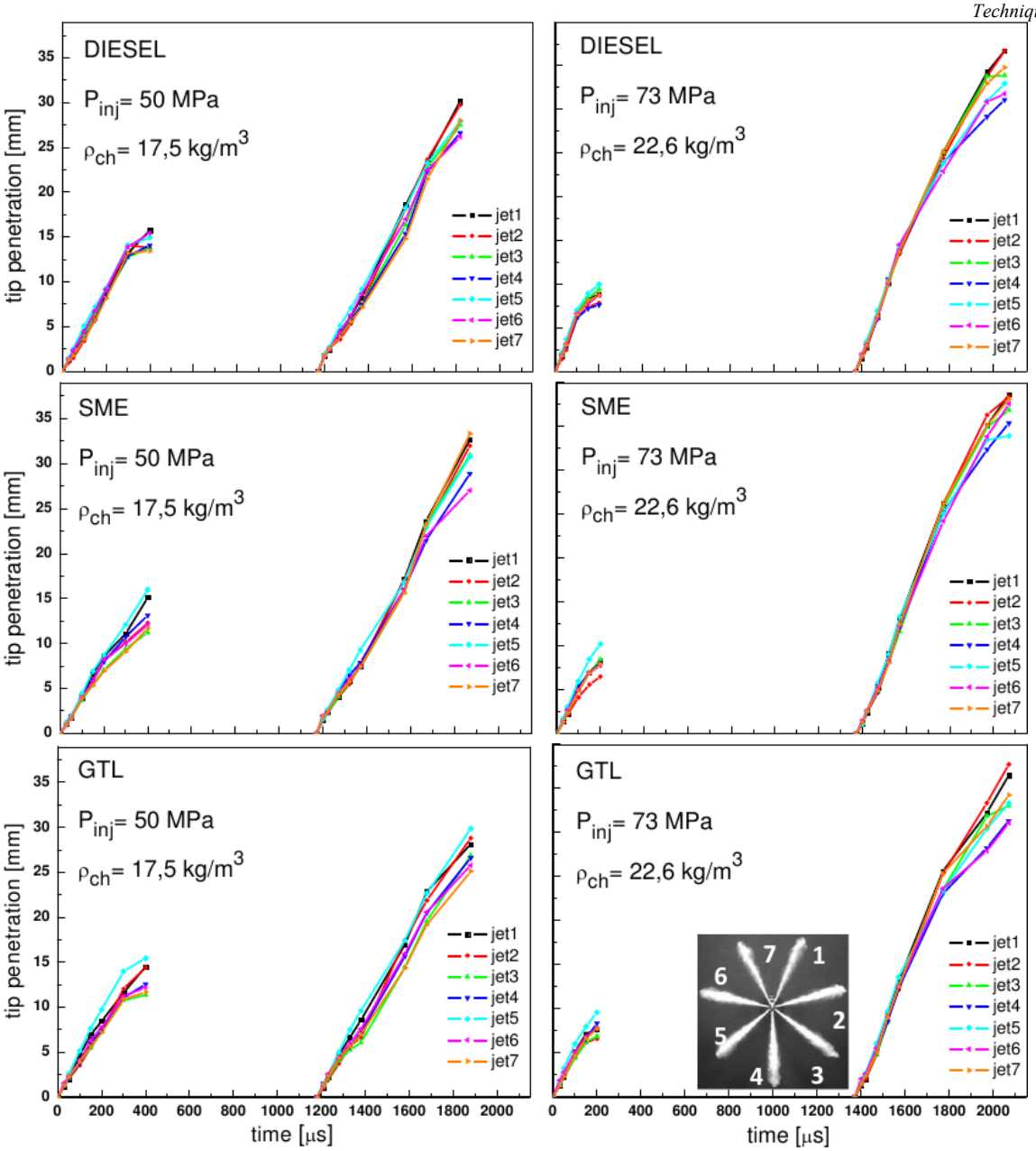

Figure 2. Individual jets penetration profiles comparison for the low load (left) and high load condition (right) in non evaporating environment

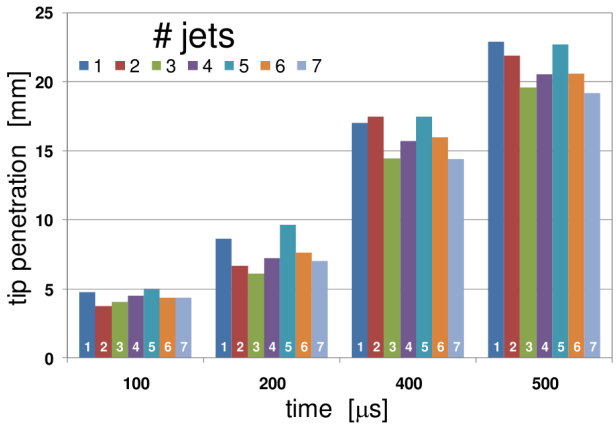

Figure 3. Tip penetration for each jet in non evaporative system, at Pinj of 50 MPa using GTL fuel

The comparisons of the tip penetration under evaporative and non evaporative conditions for the pilot and main injection, are reported in Figure 4 for both engine conditions. The curves relative at the injection pressure of 50 MPa (on the top) are split into two segments both for the pilot and the main pulses. In the first part, a good partly covering occurs for the spray penetrations for all the fuels except for the pilot of the diesel fuel. The pilot penetrations are quite similar up to 200-250 μs while the mains overlap up to 500 μs. Later a less penetrating trend for the engine evaporative conditions is shown due to the vaporization process. At the injection pressure of 73 MPa (on the bottom) the effects of the vaporization process on the main penetrations are more evident. The penetration detachments became effective around 50 μs after the start of the injection (SOI).

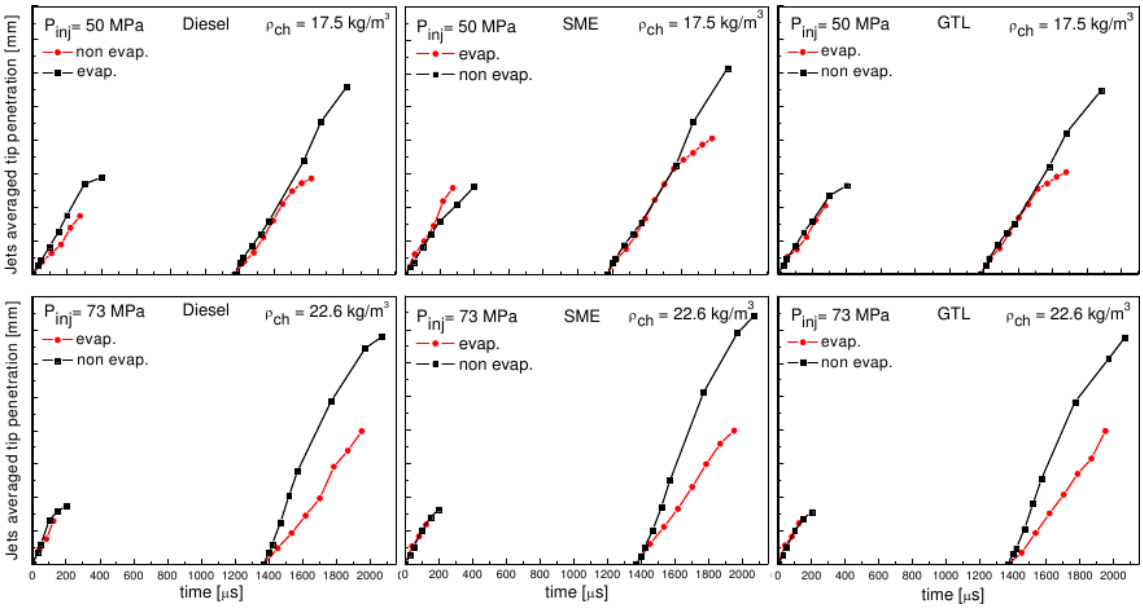

Figure 4. Comparison of liquid jet penetration profiles under evaporative (optical engine) and non-evaporative conditions

In order to better understand the liquid distribution of the several fuels, the injection images detected in the combustion chamber and in non evaporative system have been processed. The comparison has been evaluated. In particular it has been shown the analysis from the images of the injection events that occur in the non evaporative system. The background has been subtracted, the jets have been separated and converted in 8 bit images, and the iso-level lines have been detected. A scale of 256 colours has been used to represent the several luminous levels into the jet. Since fuel rich zone reflects higher percentage of light with respect to less dense zone, it is possible to recognize the fuel liquid spatial distribution.

In Figure 5 are reported the liquid spatial distribution of the jets detected in the non evaporative system at two times from the start of main injection for the high load condition (P_{inj}=73 MPa). In the graph, all jets show a liquid core and a decreasing liquid density moving towards the jets boundaries. Moreover, the SME fuel shows a denser liquid core with respect to the other ones at 400 μs and a higher penetration because of the highest density/viscosity. These results fairly agree with literature data [11].

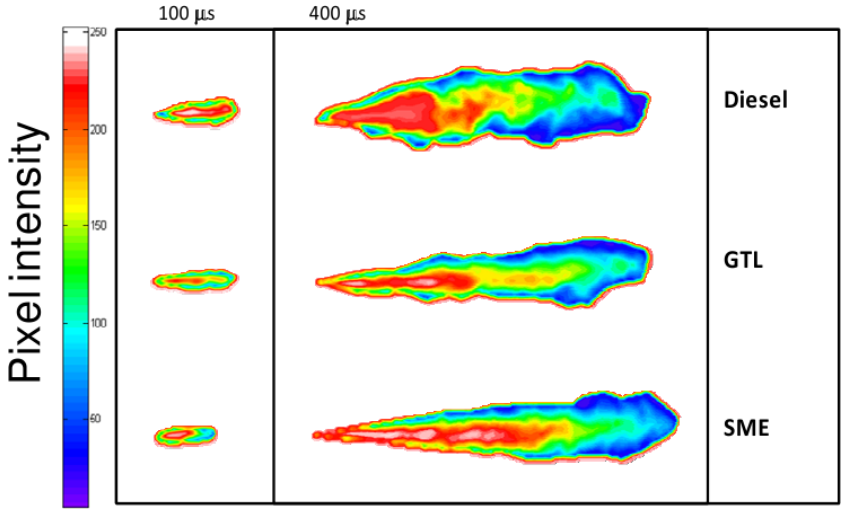

Figure 5. Jet liquid densities for the investigated fuels in non evaporative system for the high load condition (Pinj=73 MPa) at 100 µs and 400 µs after the SOI

In Figure 6 the luminous intensity detected along the jet axis during main injection for the high load condition (P_{inj}=73 MPa) are reported. The luminous intensity has been analysed at several times after the start of main injection for Diesel fuel in the optical engine and in the non evaporative system. As it can be noted, in the first case, as the penetration increases, the luminous intensity increases as well due to a higher quantity of fuel that scatters light. On the contrary, in the non evaporative system, the different experimental setup allows to reach the best illumination of the jets since the early injection. The peaks of the traces represent the Maximum Luminous Intensity Point (MLIP) of the jet axis. In the early injection it is placed near the center of the jet, then during the penetration development it starts drawing back. Physically it means that the fuel jet is mainly in liquid phase during the first stages of the injection and then it disintegrates over a finite length called the breakup length into drops of different size. The instant when the MLIP starts drawing back corresponds to the start of the breakup event.

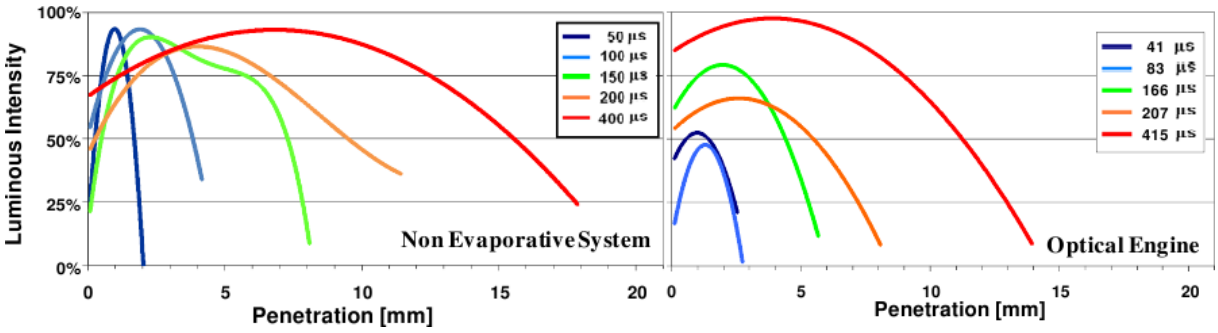

Figure 6. Luminous intensity along the jet axis for diesel fuels, for non evaporative system and optical engine at several times after the start of main injection with P_{inj} =73MPa

In Figure 7 the behaviour of the MLIP at high load condition (P_{inj} =73MPa) for all the fuels and in both non-evaporative and optical engine conditions are reported. The normalized MLIP position respect to the jet penetration (S) was plotted versus the time after the start of main injection (Main ASOI).

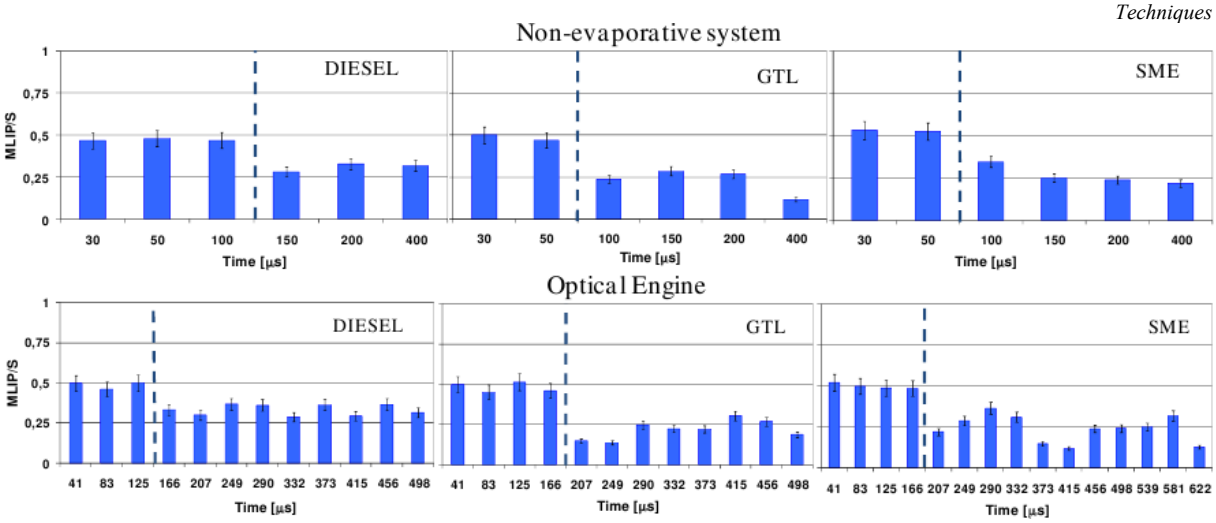

Figure 7. Normalized positions of the MLIP for the main injection in both non-evaporative and optical engine conditions (P_{inj}=73MPa)

The MLIP position is normalized with respect to the penetration and it is greater than 50% when the jet is fully liquid. When the breakup occurs, the MLIP/S ratio decreases. In the non-evaporative system the breakup occurs at 150μs, 100μs and 100μs after the start of main injection for Diesel, GTL and SME fuels, respectively. It depends on the density of the analysed fuels. In the engine the breakup occurs at 166μs, 207μs and 166μs after the start of main injection for Diesel, GTL and SME fuels, respectively. In this case, also the in-cylinder pressure and temperature strongly affect the jet behaviour in the bowl. All the breakup events in optical engine are delayed with respect to those in the non-evaporative system. In particular, even if the GTL fuel has the lowest density, it shows the delayed breakup due to the advanced combustion event that increases the in-cylinder pressure.

Conclusions

In this paper it is reported a research on the effects of alternative diesel fuels on the air/fuel mixture process, both in non evaporative and evaporative engine-like conditions. Reference diesel fuel, first and second generation biodiesels, Soybean Methyl Ether and Gas-To-Liquid, respectively, have been injected by a common rail injection system trough a 7-hole nozzle for Euro 5 engine. Fuel injection rate measurements have been carried out for the different fluids and the evolution of the spray and the fuel dispersion/vaporization have been extracted by processing the images collected in the optically accessible vessels at different times from the start of injection.

The main results on the quiescent high-pressure vessel and single-cylinder engine have put into evidence the following:

- equivalent fuel quantity is delivered at equivalent injection conditions since it is negligible the effect of the fuel chemical characteristics;
- a good stability/uniformity of jets behaviour results from the statistical analysis of their parameters in the high-pressure/room-temperature conditions, some differences in the jets penetration appear only at the lowest injection pressure and vessel gas density for Diesel and GTL main pulse due to their lowest density and viscosity;
- the penetrations are quite linear both for the pilot and the main injections for the investigated pulse durations;
- the comparison of the spray penetrations in non evaporative and evaporative conditions shows a overlapped trend for the pilot pulse, while a shorter penetration in the evaporative environment seems due to the droplet evaporation and it is more evident at high load condition;
- in both operating environments the breakup of main injection has been identified and measured; a slightly increase of breakup time has been detected due to the higher in-cylinder density during the vaporization process.

Definitions/Abbreviations

ASOI After SOI
ATDC After TDC
BTDC Before TDC
ca Crank Angle

CR Common Rail
ECU Electronic Control Unit
EGR Exhaust Gas Recirculation
GTL Gas To Liquid
MLIP Maximum Luminous Intensity Point
RME Rape Methyl Ester
TDC Top Dead Center
SME Soybean Methyl Ester
SOI Start Of Injection
VSA Variable Swirl Actuator

References

[1] Janaun, J., Ellis, N., "Perspectives on biodiesel as a sustainable fuel", Renewable and Sustainable Energy Reviews 14, pp.1312–1320, 2010
[2] Murugesan, A., Umarani, C., Subramanian, R., Nedunchezhian, N., "Bio-diesel as an alternative fuel for diesel engines-a review", Renew Sustainable Energy Rev 13 (3), pp. 653–662, 2009
[3] Lapuerta, M., Armas, O., Rodriguez-Fernandez, J., "Effect of biodiesel fuels on diesel engine emissions", Progress in Energy and Combustion Science 34, pp 198-223, 2008
[4] Allocca, L., Montanaro, A., Cipolla, G., Vassallo, A., "Spatial-Temporal Characterization of Alternative Fuel Sprays from a Second-Generation Common-Rail Fuel Injection System for Euro4 Passenger Car Application", SAE Paper 2009-01-1856, 2009
[5] He, C., Ge, Y. S., Tan, J., Han, X. K., "Spray Properties of Alternative Fuels: a Comparative Analysis of Biodiesel and Diesel", Int. J. Energy Res. 32, pp 1329-1338, 2008
[6] Gao, Y., Deng, J., Li, C., Dang, F., Liao, Z., Wu, Z., Li, L., "Experimental Study of the Spray Characteristics of Biodiesel Based on Inedible Oil", Biotechnology Advances 27, pp 616-624, 2009
[7] Allocca, L., Alfuso, S., Corcione, F. E., "Assessment of Dynamic Performances of Diesel Solenoid Injectors for a Multiple Injection Common Rail System", SAE Paper 2003-01-21, 2003
[8] Alfuso, S., Allocca, L., Caputo, G., Corcione, F. E., Montanaro, A., Valentino, G., "Experimental Investigation of a Spray from a Multi-jet Common Rail Injection System for Small Engines", SAE Paper 2005-24-090, 2005
[9] Beatrice, C., Guido, C., Vaglieco, B. M., Vassallo, A., Di Iorio, S., Mancaruso, E., "Alternative Diesel Fuels Effects on Combustion and Emissions of an Euro4 Automotive Diesel Engine", SAE Paper 2009-24-0088, 2009
[10] Mancaruso, E., Merola, S. S., Vaglieco, B. M., "Study of the multi-injection combustion process in a transparent direct injection common rail diesel engine by means of optical techniques", International Journal of Engine Research, Vol 9 - No 6, pp 483-498, 2008
[11] Allocca, L., Mancaruso, E, Montanaro, A., Vaglieco, B. M., "Alternative Diesel Fuels Characterization in Non-Evaporating and Evaporating Conditions for Diesel Engines", SAE Paper 2010-01-1516

Acknowledgments

The authors wish to thank Mr. Carlo Rossi and Bruno Sgammato for maintaining the experimental apparatus and for their precious help.